Self-Diffusion Rates in Al from Combined First-Principles and Model-Potential Calculations

Nils Sandberg,[1] Blanka Magyari-Köpe,[1] and Thomas R. Mattsson[2]
[1]*Theory of Materials, KTH-SCFAB, SE-106 91, Stockholm, Sweden*
[2]*Surface and Interface Sciences Department, MS 1415, Sandia National Laboratories, Albuquerque, New Mexico 87185-1415*
(Received 8 January 2002; published 23 July 2002)

Monovacancy diffusion alone dominates over diffusion due to divacancies and interstitials in Al for all temperatures up to the melting point. Deviations from a single Arrhenius dependence are due to anharmonicity. The conclusion is based on a combination of theoretical methods, from density functional theory to thermodynamic integration, without fitting to experimental data. The calculated diffusion rate agrees with experimental data over 11 orders of magnitude.

DOI: 10.1103/PhysRevLett.89.065901 PACS numbers: 66.30.Fq, 61.72.Ji, 71.15.Mb

Atomic scale simulations from first principles, in particular, density functional theory (DFT) [1], provide excellent information about zero-temperature properties of materials. Connecting this knowledge to the properties at the macroscopic scale and at high temperature, on the other hand, is not straightforward. In this Letter we show how this can be achieved through a combination of theoretical methods, based on atomic scale calculations without adjustable parameters.

We have focused on the specific case of vacancy migration in Al. Vacancy migration is the dominating mechanism for self-diffusion in most elemental crystals and has been extensively studied. Much is known [2–4], but the detailed interpretation of high-temperature data is intrinsically difficult and open questions remain. For instance, the contribution from more mobile defects, i.e., divacancies and interstitials, to the diffusion process, and the role of anharmonicity in the atomic vibrations need to be simultaneously considered. In theoretical calculations claiming predictive power, this should be done without fitting to experimental data.

Combining several theoretical methods, we show that the self-diffusion in Al is solely due to vacancy migration, for all temperatures up to the melting temperature, an explanation that has been under debate [2,5,6]. We obtain the effective high-temperature diffusion barrier to within 5% of the experimental value. There is also an excellent agreement with the absolute diffusion rate, D. Our work extends previous calculations of the vacancy concentration, c_v, in Al [7]. That work showed that the divacancy is energetically unstable at $T = 0$ K and unnecessary for the understanding of vacancy concentration data. It may still (like the interstitial) contribute to the self-diffusion at high T if the migration free energy is sufficiently low and is therefore included in the present analysis. After giving the basic definitions, we in detail describe the computational methods used, in particular, how they are connected, before presenting the results.

The equilibrium concentration c of a defect at zero pressure is governed by a formation enthalpy, H^f, and a formation entropy, S^f,

$$c = g^f e^{S^f/k_B - H^f/k_B T}, \quad (1)$$

where T is the temperature, k_B is Boltzmann's constant, and g^f is a geometrical factor. The defect migration rate Γ is

$$\Gamma = g^m \Gamma_0 e^{-H^m/k_B T}, \quad (2)$$

where H^m is a migration enthalpy, Γ_0 is an attempt frequency that may be expressed in terms of a migration entropy, and g^m is a geometrical factor. At elevated temperatures, H^f, H^m, S^f, and Γ_0 are in general temperature dependent. The connection with static quantities is made through lattice dynamics theory and transition-state theory (TST) [8]. Assuming harmonic vibrations, H^m then is given by the relaxed transition-state energy (relative to the defect state) and H^f by the relaxed defect state energy (relative to the bulk). The diffusion barrier, $H^D = H^f + H^m$, is thus possible to calculate directly using first-principles methods. With some more effort, S^f and the TST prefactor Γ_0^{TST} are obtained from vibrational frequencies in the transition state, defect and bulk systems. A first-principles calculation of the diffusion rate, using harmonic TST, has been reported for, e.g., Li [9].

We begin with presenting DFT calculations of the formation enthalpies for the vacancy, the divacancy, and the ⟨100⟩-dumbbell interstitial, and of the migration enthalpy for the vacancy, in Al. Defect formation parameters were obtained by comparing relaxed defect and bulk systems at zero pressure. The transition state was found by the nudged elastic band method [10], at constant volume. The calculations used VASP [11], a code well suited for computational materials physics. The Kohn-Sham equations [1] are solved in a plane-wave basis set, and the ions are described using ultrasoft pseudopotentials [12]. We used the PW91 functional [13], a generalized gradient approximation (GGA), because of its properties for bulk Al [7]. Most DFT calculations reported here were done in a unit cell with $4 \times 4 \times 5$ lattice points. The bulk cell thus include 80 atoms, the vacancy cell 79 atoms, the divacancy cell 78 atoms, and the interstitial cell 81 atoms. Convergence tests were performed for the vacancy (using cells consisting of 32, 80, 108, and 125 lattice points) and for the

TABLE I. Convergence test for Al vacancy and interstitial.

Cell size	E_v (eV)	E_i (eV)
32	0.52	
80	0.54	2.43
108	0.54	2.43
125	0.54	

interstitial (80 and 125 lattice points); see Table I. The convergence tests show that the 80 lattice-point cell is large enough for our purpose. The Brillouin zone was sampled using a $4 \times 4 \times 4$ mesh of k points and the cutoff energy for the plane-wave coefficients was 130 eV. Given the size of the system in real space and the ultrasoft pseudopotentials these choices ensure that the electronic structure is converged.

The difference between propagating and evanescent wave functions causes both GGA and local density approximation to make errors at surfaces [14], and *the error in energy is proportional to the surface area.* Evanescent wave functions occur at a vacancy, making it necessary to adjust vacancy formation energies [7]. Mattsson and Kohn [14] have formulated a correction scheme for this error by using a reference system; a suitable reference is the half-jellium system [15]. We correct the vacancy migration energy by estimating the difference in exposed surface area between the transition state and the minimum energy state. At the transition state the migrating atom divides the ''vacancy volume'' into two pieces. Assuming that the volume is kept constant the area depends on the geometry of the two voids. The calculated GGA value for the vacancy migration barrier is 0.545 eV and the corrected H_v^m is 0.60 ± 0.02 eV, with the estimated error stemming from the area at the transition state [16].

At high temperatures ($T > T_m/2$, T_m being the melting point), anharmonicity in the interatomic forces makes the formation and migration enthalpies temperature dependent. To deal with this, and to obtain formation and migration entropies, we used the Ercolessi-Adams (EA) model potential [18] (MP) of the pair-functional form [19], which implies central forces. Al is a free electron metal where directional bonds are important only at very low coordination numbers (three), affecting, for example, surface diffusion [20]. Modeling metals with directed bonds also in the bulk requires more elaborate potentials, thus increasing the computational demands. The potential used here is fitted to first-principles data for bulk and defect systems, at zero and finite temperatures. It should, therefore, be well suited for extending our first-principles results to include thermal properties. Table II confirms that the MP well describes key properties of divacancies and interstitials, which were not included in the fitting of the potential.

We calculated the low-temperature defect formation entropies and TST prefactors via the eigenvalues of the force-constant matrix [8,21]. Standard routines were used to keep zero pressure. Most of these calculations were done for systems consisting of 500 lattice points. Those values, and DFT and MP formation and migration enthalpies, valid in the harmonic approximation, are presented in Table II. The concentration dependence of the formation parameters was estimated by repeating the calculations for the vacancy and the interstitial in 2048 lattice-point systems. Compared with the values given in Table II, H_v^f and S_v^f differed with 4×10^{-4} eV and $0.02k_B$, while H_i^f and S_i^f differed with 0.007 eV and $-0.09k_B$. We conclude that, for the small concentrations at hand, the defects may be treated as noninteracting. For the vacancy migration barrier, a MP calculation performed at constant volume gave a difference of 5×10^{-4} eV, showing that the correction to the DFT value due to the choice of boundary conditions is small.

We now proceed with considering the temperature dependencies of the defect formation enthalpies, obtained in long molecular dynamics (MD) simulations of isolated defects. Constant temperature and zero pressure conditions were achieved using standard techniques [22,23]. During such a simulation the defect will migrate, and jump frequencies can be derived simultaneously. The divacancy migrates by one of the four atoms surrounding the divacancy's ''waistline'' jumping into a vacant site. However, occasionally, one of the other 14 atoms surrounding the divacancy will perform a jump, thus leading to divacancy splitting. In our simulations, this was avoided by monitoring a set of reaction coordinates $\xi_i = (\bar{r}_i - \frac{1}{4}\sum_{j=1}^{4} \bar{r}_j)\bar{e}_i$, where i refers to one of the 14 atoms, j to the four atoms that constitute the bottleneck for the jump into the vacant site, and $\bar{e}_i$ to the jump direction. When any ξ exceeded 0, it was reflected back by applying a harmonic force. Calculated temperature dependencies of H^f are presented in Fig. 1. The result for vacancies essentially reproduces the one in Ref. [7]. The other curves show a similar trend, but we note that the anharmonic increase in the interstitial

TABLE II. Defect formation enthalpies H^f and entropies S^f, migration enthalpies H^m, and rate prefactors Γ_0^{TST} calculated in the harmonic approximation, and compared with experiments [17]. Data for vacancies (v), divacancies (2v), and interstitials (i) are given in units of eV for enthalpies, k_B for entropies, and the Debye frequency $\Gamma_{Debye} = 8.4$ THz for rate prefactors.

	H_v^f	S_v^f	H_v^m	$\Gamma_{0,v}^{TST}$	H_{2v}^f	S_{2v}^f	H_{2v}^m	$\Gamma_{0,2v}^{TST}$	H_i^f	S_i^f	H_i^m	$\Gamma_{0,i}^{TST}$
DFT/GGA	0.69 [7]		0.60 ± 0.02		1.46 [7]				2.43			
MP/EA	0.69	1.14	0.61	2.69	1.38	2.50	0.27	2.01	2.47	5.19	0.16	0.40
exp.	0.68	0.7	0.61 ± 0.03				0.50		3.0		0.115	

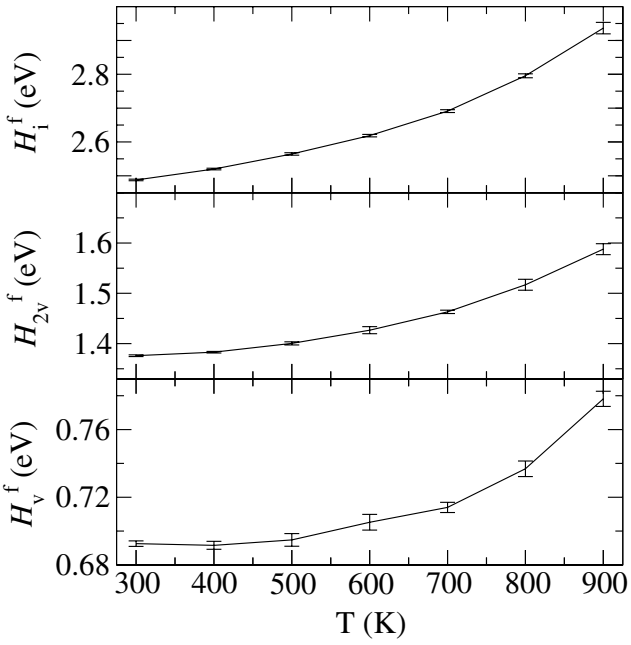

FIG. 1. Formation enthalpies for vacancies (v), divacancies (2v), and interstitials (i), obtained in MD simulations.

formation enthalpy transfers to a large increase in effective entropy [$S_i^f(T = T_m) \approx 9k_B$]. This is believed to be a general feature of the interstitial [24].

Defect concentrations were calculated by integrating the relation $\frac{\partial H}{\partial T} = T\frac{\partial S}{\partial T}$ from $T = 0$, where the constant of integration is given by S^f in Table II.

Defect migration rates were obtained by continuously keeping track of the position of the defect during the MD simulations [5]. To do this unambiguously, copies of the system were repeatedly quenched and each atom was assigned to a lattice point. This quenching was triggered by monitoring suitably selected reaction coordinates. For the vacancy, for instance, ξ_i defined as above, for the 12 atoms surrounding the vacancy was monitored. If any ξ exceeded $l/4$, it was regarded as a jump, a copy of the system was relaxed, and new lattice points and ξ's were found. This procedure did not affect the evolution of the simulation. Divacancy and interstitial migration rates were obtained similarly.

At temperatures below about $0.75T_m$, the vacancy jump frequency is too low for ''direct'' simulations to be feasible. We then used a thermodynamic integration (TI) technique, as described by Boisvert *et al.* [25], which accounts for return jumps as well as anharmonicity. The free energy required to bring the jumping atom adiabatically from the initial state to the transition state was calculated in 100 steps over a total of 2–4 ns. In these simulations the other atoms were prevented from jumping into one of the ''half vacancies'' by a technique similar to that used in the divacancy simulations. At the highest temperatures used here, this occurred with an average interval of 25 ps. It should not affect the results significantly. Separate calculations with the system constrained at $\xi = 0$ were also carried out. In intervals of 2 ps the constraint was released and ξ was followed both forwards and backwards in time. Inspection of the jump trajectories showed that $\kappa = 0.8$ and does not vary notably with temperature.

Defect migration frequencies calculated within the harmonic TST and in direct simulations, and vacancy migration rates calculated indirectly through TST/TI, are presented in Fig. 2. The temperature ranges for the direct vacancy simulations and the TST/TI calculations overlap at $T = 750$, 800, and 850 K, thereby allowing a direct comparison between the methods. The agreement is excellent, with deviations less than 5% in Γ_v (see the inset in Fig. 2), in line with previous results [25].

Finally, we calculate the macroscopic diffusion rate of a marked tracer atom as $D^{tr} = \frac{1}{6}l^2 f c\Gamma$, where the correlation factor f equals 0.78, 0.49, and 0.44 for vacancies, divacancies and interstitials, respectively [26,27]. The calculated diffusion rate D^{tr} is shown in Fig. 3. The contribution from divacancies and interstitials is less than 1% of that from vacancies at the melting point. Vacancy migration is seen to explain the measured tracer diffusion rates to within a factor of 2. The discrepancy corresponds to an error of 0.05 eV in the thermal barrier H^D, which is comparable to the estimated error in our first-principles calculation of H_v^m. The anharmonic increase in H^D from $T = 0$ to $T = T_m$ is

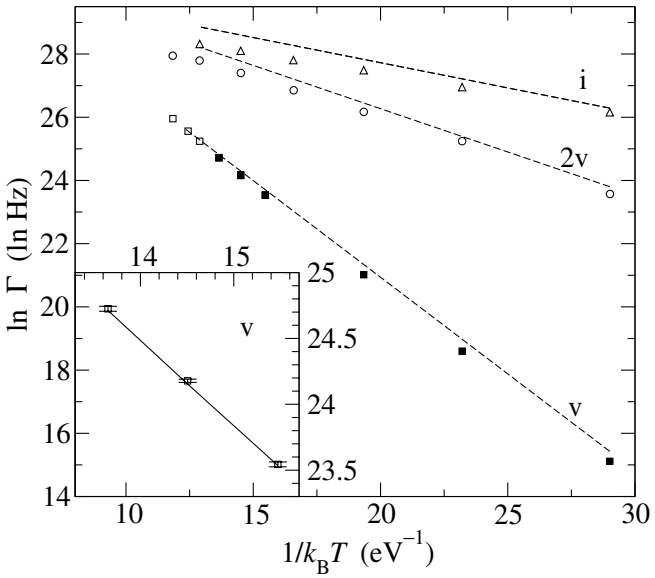

FIG. 2. Jump frequencies, Γ, for vacancies (v), divacancies (2v), and interstitials (i) from direct MD simulations (open symbols). Estimated errors are smaller than the symbols. Dashed lines indicate harmonic TST rates and filled squares are TST/TI results for vacancies. The region of overlap between direct MD and TST/TI calculations is shown in the inset. The solid line connects the TST/TI calculations performed at the same temperatures as the direct simulations.

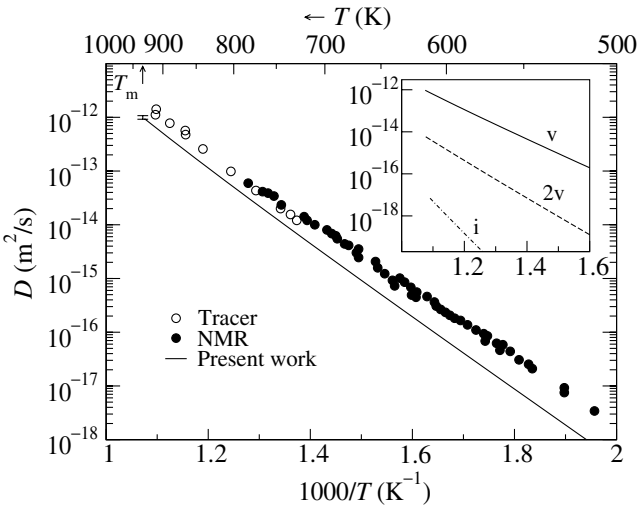

FIG. 3. Self-diffusion constants, obtained in model potential MD simulations. Open and filled circles are experimental data [3]. The inset shows calculated diffusion constants for vacancies (v), divacancies (2v), and interstitials (i). The contribution from divacancies and interstitials is less than 1% of that from vacancies at the melting point.

about 10%, leading to a high-temperature value of 1.43 eV, to be compared with the experimental value 1.48 eV.

The significant discrepancy between tracer diffusion data and nuclear magnetic resonance (NMR) data (see Fig. 3) has been discussed in detail in Ref. [6]. The authors did not arrive at a definite conclusion. Our calculations strongly support the tracer diffusion data. We also note that our calculated D^{tr} agree to within a factor of 2 with low-temperature diffusion data (350 K $< T <$ 500 K) based on transmission electron microscope observation of void shrinkage [3].

In conclusion, we have found that the monovacancy alone accounts for measured self-diffusion constants in Al, for all temperatures up to the melting point. Our calculations agree with experimental data spanning 11 orders of magnitude and, more importantly, add key new insights into the diffusion processes. This shows the prospect of modeling macroscopic, high-temperature processes by combining different theoretical methods.

We thank K. Carling, G. Grimvall, A. E. Mattsson, and G. Wahnström for helpful discussions. This work was supported by the Swedish research organization SSF. T. R. M. acknowledges support from the Motorola/SNL computational materials CRADA. Sandia is a multiprogram laboratory operated by Sandia Corporation, a Lockheed Martin Company, for the United States Department of Energy under Contract No. DE-AC04-94AL85000.

[1] P. Hohenberg and W. Kohn, Phys. Rev. **136**, B864 (1964); W. Kohn and L. J. Sham, Phys. Rev. **140**, A1133 (1965).
[2] N. L. Peterson, J. Nucl. Mater. **69–70**, 3 (1978).
[3] H. Mehrer, N. Stolica, and N. A. Stolwijk, in *Diffusion in Solid Metals and Alloys, Landolt-Börnstein*, New Series, Group III, Vol. 26 (Springer-Verlag, Berlin, 1990).
[4] Y. Kraftmakher, Phys. Rep. **299**, 79 (1998).
[5] K. Nordlund and R. S. Averback, Phys. Rev. Lett. **80**, 4201 (1998).
[6] S. Dais, R. Messer, and A. Seeger, Mater. Sci. Forum **15–18**, 419 (1987).
[7] K. Carling *et al.*, Phys. Rev. Lett. **85**, 3862 (2000).
[8] G. H. Vineyard, J. Phys. Chem. Solids **3**, 121 (1957).
[9] W. Frank, U. Breier, C. Elsässer, and M. Fähnle, Phys. Rev. Lett. **77**, 518 (1996).
[10] G. Mills, H. Jónsson, and G. K. Schenter, Surf. Sci. **324**, 305 (1995).
[11] G. Kresse and J. Hafner, Phys. Rev. B **47**, 558 (1993); **49**, 14 251 (1994); G. Kresse and J. Furthmüller, Phys. Rev. B **54**, 11 169 (1996).
[12] D. Vanderbilt, Phys. Rev. B **41**, 7892 (1990); G. Kresse and J. Hafner, J. Phys. Condens. Matter **6**, 8245 (1994).
[13] J. P. Perdew *et al.*, Phys. Rev. B **46**, 6671 (1992); **48**, 4978 (1993).
[14] A. E. Mattsson and W. Kohn, J. Chem. Phys. **115**, 3441 (2001).
[15] S. Kurth, J. P. Perdew, and P. Blaha, Int. J. Quantum Chem. **75**, 889 (1999).
[16] Without this correction, GGA, as well as LDA, gives values outside the experimental interval, 0.61 ± 0.03 eV [17].
[17] P. Ehrhart, in *Properties and Interactions of Atomic Defects in Metals And Alloys*, Landolt-Börnstein, New Series, Group III, Vol. 25 (Springer-Verlag, Berlin, 1991).
[18] F. Ercolessi and J. B. Adams, Europhys. Lett. **26**, 583 (1994).
[19] The form of this potential is equivalent to that of, e.g., the embedded atom model potentials; see A. E. Carlsson, in *Solid State Physics* (Academic Press, Boston, 1990), Vol. 43.
[20] P. J. Feibelman, Phys. Rev. Lett. **65**, 729 (1990).
[21] S. M. Foiles, Phys. Rev. B **49**, 14 930 (1994).
[22] W. G. Hoover, Phys. Rev. A **31**, 1695 (1985).
[23] M. Parrinello and A. Rahman, Phys. Rev. Lett. **45**, 1196 (1980).
[24] A. V. Granato, Phys. Rev. Lett. **68**, 974 (1992).
[25] G. Boisvert, N. Mousseau, and L. J. Lewis, Phys. Rev. B **58**, 12 667 (1998).
[26] D. Wolf, Philos. Mag. A **47**, 147 (1983).
[27] The relation is strictly valid only for spatially uncorrelated defect jumps. Correlations were found in the case of interstitial migration close to T_m. However, explicit comparisons with the total atom displacement during a simulation showed that this correlation had a minor effect on the atomic diffusion rate.